ACS OMEGA

http://pubs.acs.org/journal/acsodf

Article

Synthesis and Properties of Short-Lifetime Thermally Activated Delayed Fluorescence Materials

Liang Zhang,* Dingding Yang, Quanxing Li, Zhi-Jun Li, Wen-Bo Zhu, Kejian Chang, Haiyan Song, and Chuan-Feng Chen*

Cite This: *ACS Omega* 2023, 8, 23142−23147

Read Online

ACCESS | Metrics & More | Article Recommendations | Supporting Information

ABSTRACT: Compounds **MBZ-mPXZ**, **MBZ-2PXZ**, **MBZ-oPXZ**, **EBZ-PXZ**, and **TBZ-PXZ** were conveniently synthesized, and they were found to exhibit TADF properties with lifetimes of 857, 575, 561, 768, and 600 ns, respectively. These short lifetimes of the compounds might be due to the combination of small singlet−triplet splitting energy (ΔE_{ST}) and benzoate group, which could be an efficient strategy for the further design of short-lifetime TADF materials.

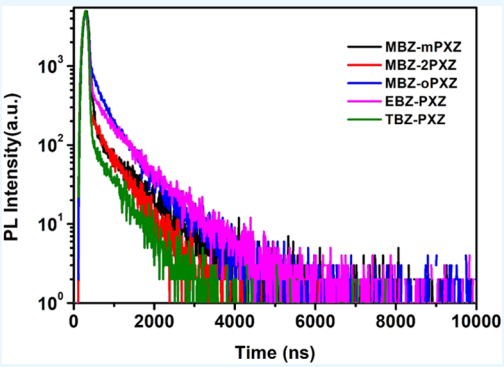

INTRODUCTION

Since the first report of pure organic thermally activated delayed fluorescence (TADF) emitter,[1] TADF materials have aroused increasing interest, and thus have also become the third-generation organic luminescent materials[2,3] after fluorescent[4−6] and phosphorescent materials.[7] As the third-generation organic luminescent material, TADF is a special radiative transition via reverse intersystem crossing (RISC) of excitons from the lowest triplet (T_1)[8−10] to the lowest singlet (S_1) state,[11] and thus obtain a high theoretical quantum yield of 100%.[12,13] Generally, TADF molecules are designed by introducing a twisted angle between acceptor[14] and donor moieties[15,16] to avoid the overlap between the lowest unoccupied molecular orbital (LUMO)[17] and the highest occupied molecular orbital (HOMO).[18] So far, various electron-accepting moieties have been applied as receptors for the design and construction of TADF molecules.[19] However, benzoate groups have rarely been used as receptors to study their TADF property.

The delayed lifetime of TADF materials is in the range of hundreds of microseconds as a result of their endothermic RISC process.[20] Most of TADF materials reveal a long delayed fluorescent lifetime,[21,22] which leads to enhancement of the triplet-related nonradiative process,[23−26] such as triplet−triplet annihilate (TTA), triplet-polaron annihilate (TPA), and severe efficiency roll-off at a high current density.

Herein, we report a novel kind of organic luminescent materials **MBZ-mPXZ**, **MBZ-2PXZ**, **MBZ-oPXZ**, **EBZ-PXZ**, and **TBZ-PXZ** (Figure 1) containing a benzoate group and a phenoxazine subunit, which not only showed TADF property in films but also exhibited a shorter lifetime. Especially, short-lifetime thermally activated delayed fluorescence materials would be used as promising luminescent materials for organic light-emitting diodes.

RESULTS AND DISCUSSION

Synthesis and Characterization. The synthetic routes of compound **MBZ-oPXZ** are shown in Scheme 1. Compound **MBZ-oPXZ** was conveniently synthesized in good yields by palladium-catalyzed cross-coupling reactions of methyl 2-bromobenzoate with phenoxazine, respectively. Similar synthetic steps were followed for other compounds. The compounds **MBZ-mPXZ**, **MBZ-2PXZ**, **MBZ-oPXZ**, **EBZ-PXZ**, and **TBZ-PXZ** could be easily synthesized in good yield. Their structures were confirmed by ^{1}H NMR, ^{13}C NMR, and HRMS spectra.

Photophysical Properties. The UV−vis absorption spectra of **MBZ-mPXZ**, **MBZ-2PXZ**, **MBZ-oPXZ**, **EBZ-PXZ**, and **TBZ-PXZ** in tetrahydrofuran are shown in Figure 2a. Owing to their similar structures, the absorption bands of the five compounds are similar. These compounds showed broad absorption bands 317 and 324 nm, which were assigned

Received: April 16, 2023
Accepted: June 2, 2023
Published: June 15, 2023

https://doi.org/10.1021/acsomega.3c02595
ACS Omega 2023, 8, 23142−23147

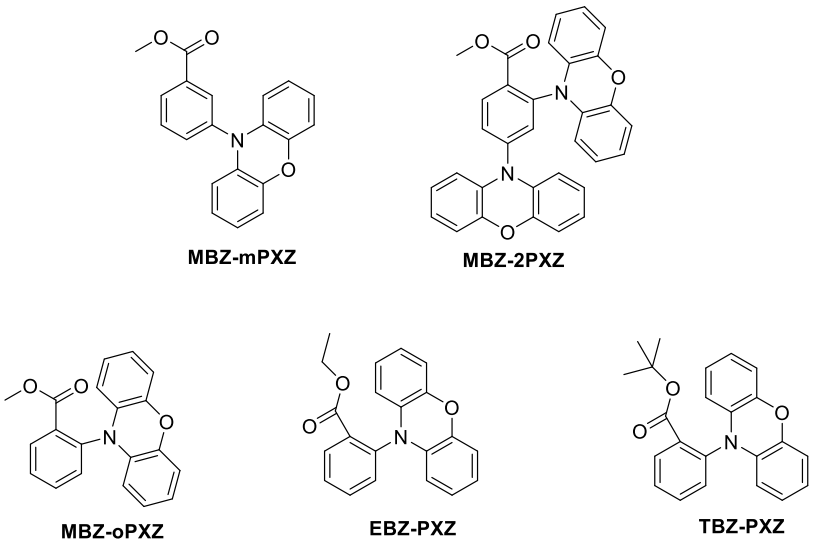

Figure 1. Structures of **MBZ-mPXZ**, **MBZ-2PXZ**, **MBZ-oPXZ**, **EBZ-PXZ**, and **TBZ-PXZ**.

Scheme 1. Synthesis of the MBZ-mPXZ Compound

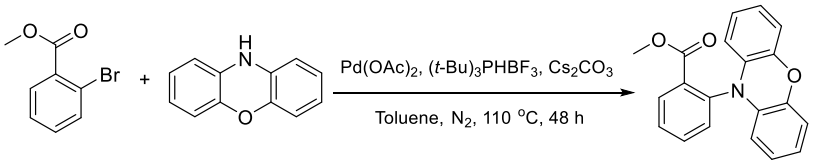

to $\pi-\pi^*$ transitions. Their absorption band range of 396 nm can be assigned to the strong intermolecular charge transfer (ICT) between the phenoxazine donor moieties and the benzoate acceptor group. As shown in Figure 2b, we can achieve color regulation by regulating the strength of ICT transition. The maximum fluorescence emission peaks are red-shifted with an increase of the donor's electron-donating ability, and are 498 and 536 nm for **MBZ-mPXZ** and **MBZ-2PXZ**, respectively. In addition, TADF materials with the same donor and different acceptors were studied. When the acceptors were methyl benzoate, ethyl benzoate, and tert-butyl benzoate, their fluorescence emission showed similar properties. The fluorescence peaks of **MBZ-oPXZ**, **EBZ-PXZ**, and **TBZ-PXZ** were centered at 510, 510, and 509 nm in films, respectively. Absolute PLQYs of **MBZ-mPXZ**, **MBZ-2PXZ**, **MBZ-oPXZ**, **EBZ-PXZ**, and **TBZ-PXZ** in films were 62.55, 54.69, 74.69, 59.42, and 78.74%, respectively. The chromatic coordinates of these luminescent compounds have also been studied. For **MBZ-mPXZ** and **MBZ-2PXZ**, their fluorescence CIE coordinates were found to be at (0.22, 0.44) and (0.37, 0.58), respectively. Simultaneously, the fluorescence CIE coordinates of **MBZ-oPXZ**, **EBZ-PXZ**, and **TBZ-PXZ** were at (0.26, 0.50), (0.27, 0.50), and (0.26, 0.51), respectively.

The transient PL spectra of **MBZ-mPXZ**, **MBZ-2PXZ**, **MBZ-oPXZ**, **EBZ-PXZ**, and **TBZ-PXZ** in films were further conducted to determine whether the triplet excited states were involved in the delayed luminescence. As shown in Figure 3, it was found that the DF lifetimes of **MBZ-mPXZ**, **MBZ-2PXZ**, **MBZ-oPXZ**, **EBZ-PXZ**, and **TBZ-PXZ** in neat films at room temperature were 857, 575, 561, 768, and 600 ns, respectively. It was found that these compounds displayed a distinctive microsecond-scaled delayed relaxation at room temperature, which implied the TADF properties of the emitters.

Single-Crystal Analyses. To obtain more insights into the TADF property of molecular conformations and the crystal packing of **MBZ-mPXZ** and **MBZ-oPXZ**, their single-crystal structures were obtained. These single-crystal structures were grown from dichloromethane/petroleum ether by slow solvent evaporation. As illustrated in Figure 4, the emitter adopted a highly twisted conformation with dihedral angles between the benzoate group and phenoxazine subunit in **MBZ-oPXZ** of 86.75°. Similarly, the dihedral angle between the donor and the acceptor of **MBZ-mPXZ** is 77.34°. The nearly vertical donor–acceptor linkage is conductive to the efficient separation of the HOMO/LUMO and low electronic coupling, leading to small ΔE_{ST} and subsequently efficient TADF property.[27] Besides, the crystal packing of **MBZ-mPXZ** and **MBZ-oPXZ** was also investigated. As shown in Figures S1 and S2, Supporting Information, we also found that compared with **MBZ-mPXZ**, **MBZ-oPXZ** showed molecular packing in a compact pattern because of the more twisted conformation. Moreover, **MBZ-oPXZ** and **MBZ-mPXZ** formed a multiple network structure due to the C–H···O (2.53–2.635 Å) and C–H···π (2.843–2.858 Å) intermolecular interactions, which might be powerful to restrict molecular motions and suppress the nonradiative decay.

DFT Calculations. The density functional theory (DFT) calculation for all molecules was performed using GAUSSIAN 09W package.[28] All of the molecules were optimized following the Becke-3–Yang–Parr (B3LYP) functional combined with the basis set of def2-SVP (Ahlrich split-valence basis set with polarization functions on heavy atoms). Note that the dispersion corrections for the nonbonding vdW interaction were carried out through the Grimme approach using atom pair-wise additive schemes, the so-called DFT-D3 method. Finally, the excited states of all optimized structures were further investigated at the accuracy level of wB97XD/TZVP.

https://doi.org/10.1021/acsomega.3c02595
ACS Omega 2023, 8, 23142–23147

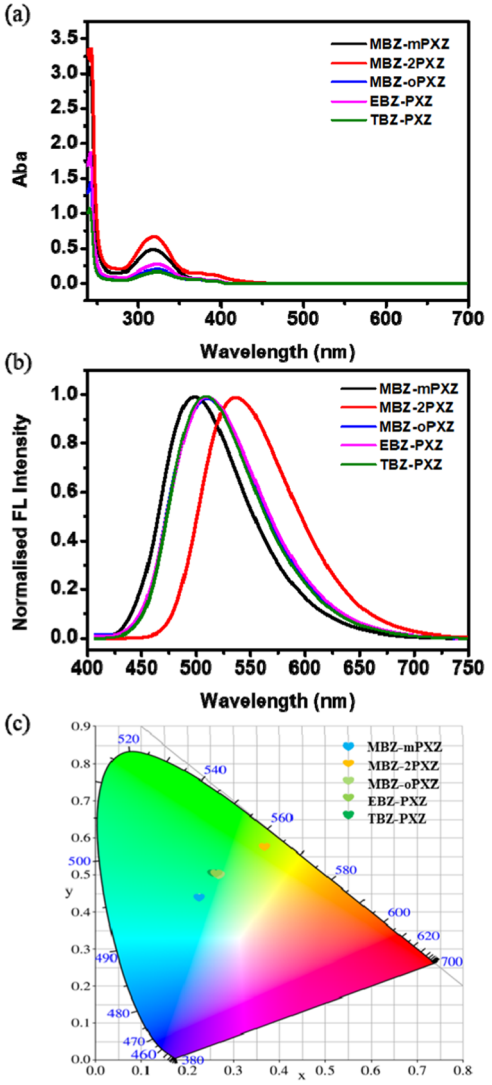

Figure 2. (a) Absorption spectra of **MBZ-mPXZ**, **MBZ-2PXZ**, **MBZ-oPXZ**, **EBZ-PXZ**, and **TBZ-PXZ** in tetrahydrofuran at room temperature. (b) Fluorescence spectra of **MBZ-mPXZ**, **MBZ-2PXZ**, **MBZ-oPXZ**, **EBZ-PXZ**, and **TBZ-PXZ** in neat films at room temperature. (c) CIE coordinates of the PL (CIE 1931 Chromaticity Coordinate Calculation).

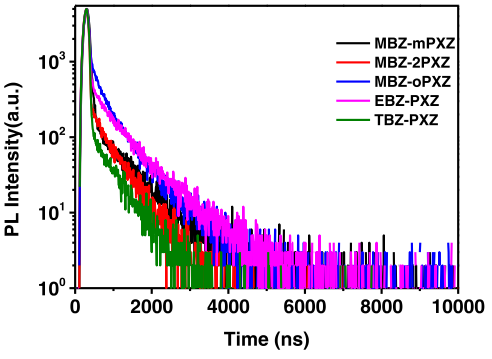

Figure 3. Transient decay spectra of **MBZ-mPXZ**, **MBZ-2PXZ**, **MBZ-oPXZ**, **EBZ-PXZ**, and **TBZ-PXZ** in a neat film at room temperature.

The optimized geometry and the electron density distribution of **MBZ-mPXZ**, **MBZ-2PXZ**, **MBZ-oPXZ**, **EBZ-PXZ**, and **TBZ-PXZ** were investigated by density functional theory calculations (Figure 5). Five compounds all showed the separated HOMO and LUMO distributions on their optimized geometries. The HOMOs are predominantly located on the electron-donating phenoxazine subunit, whereas the LUMOs are distributed over the electron-withdrawing benzoate group. The frontier molecular orbital of **MBZ-mPXZ**, **MBZ-2PXZ**, **MBZ-oPXZ**, **EBZ-PXZ**, and **TBZ-PXZ** showed small overlap mainly on the donor and acceptor units, resulting in the appreciable ΔE_{ST} values, evidenced by the calculated ΔE_{ST} values of 0.0717, 0.0143, 0.0222, 0.0497, and 0.0570 eV, respectively. Small ΔE_{ST} values led to the high efficiency of the RISC, which could induce the TADF capability.

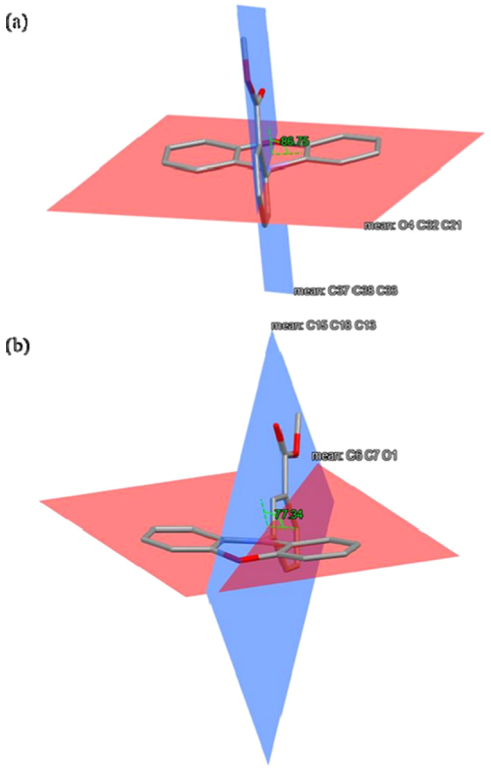

Figure 4. Crystal structures of (a) **MBZ-oPXZ** and (b) **MBZ-mPXZ**.

CONCLUSIONS

In conclusion, we have conveniently synthesized compounds **MBZ-mPXZ**, **MBZ-2PXZ**, **MBZ-oPXZ**, **EBZ-PXZ**, and **TBZ-PXZ** and found that they exhibited TADF properties with lifetimes of 857, 575, 561, 768, and 600 ns, respectively. By connecting the donor group with the benzoate unit, we achieved effective separation between HOMO and LUMO. The negligible overlap between HOMO and LUMO enables its CT character and a small ΔE_{ST}. The small ΔE_{ST} facilitates fast RISC process and reduces the delayed fluorescence lifetime. Their short lifetime might be due to the combination of small ΔE_{ST} and benzoate group, which may provide a new way and an efficient strategy for the further design of short-lifetime TADF materials.

EXPERIMENTAL SECTION

Synthesis of MBZ-mPXZ. A mixture of $Pd(OAc)_2$ (44 mg, 0.2 mmol), Cs_2CO_3 (977 mg, 3.0 mmol), $(t\text{-Bu})_3PHBF_4$ (88 mg, 0.3 mmol), methyl 3-bromobenzoate (677 mg, 2.7 mmol), and 10H-phenoxazine (458 mg, 2.5 mmol) in toluene (20 mL)

https://doi.org/10.1021/acsomega.3c02595
ACS Omega 2023, 8, 23142−23147

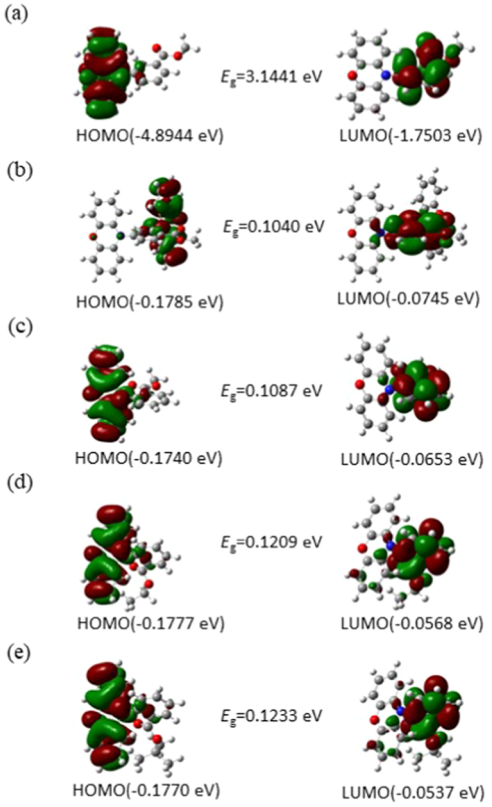

Figure 5. Calculated spatial distributions of the HOMO and LUMO energy densities of (a) **MBZ-mPXZ**, (b) **MBZ-2PXZ**, (c) **MBZ-oPXZ**, (d) **EBZ-PXZ**, and (e) **TBZ-PXZ**.

was refluxed under N_2 for 48 h. After cooling to room temperature, the reaction mixture was filtered and the residue was purified by column chromatography on silica gel to give a yellow powder (682 mg, yield 86%). Mp: 143−144 °C. ^{1}H NMR (400 MHz, $CDCl_3$) δ 8.16 (d, J = 7.6 Hz, 1H), 8.05 (s, 1H), 7.68 (t, J = 7.8 Hz, 1H), 7.57 (d, J = 7.6 Hz, 1H), 6.77−6.63 (m, 4H), 6.59 (dd, J = 10.8, 4.1 Hz, 2H), 5.86 (d, J = 7.6 Hz, 2H), 3.93 (s, 3H). ^{13}C NMR (101 MHz, $CDCl_3$) δ 166.09 (s), 143.93 (s), 139.37 (s), 135.86 (s), 134.04 (s), 133.42 (s), 132.39 (s), 131.28 (s), 129.70 (s), 123.29 (s), 121.64 (s), 115.61 (s), 113.23 (s), 77.37 (s), 77.05 (s), 76.73 (s), 52.42 (s). HRMS (APCI) m/z: $[M + H]^+$ calcd for $C_{20}H_{15}NO_3$, 317.1052; found, 318.1112.

Synthesis of MBZ-2PXZ. A mixture of $Pd(OAc)_2$ (44 mg, 0.2 mmol), Cs_2CO_3 (977 mg, 3.0 mmol), (t-Bu)$_3$PHBF$_4$ (88 mg, 0.3 mmol), methyl 2,4-dibromobenzoate (292 mg, 1.0 mmol), and 10H-phenoxazine (366 mg, 2.0 mmol) in toluene (20 mL) was refluxed under N_2 for 48 h. After cooling to room temperature, the reaction mixture was filtered and the residue was purified by column chromatography on silica gel to give a yellow powder (697 mg, yield 70%). Mp: 210−211 °C. ^{1}H NMR (400 MHz, $CDCl_3$) δ 8.35 (d, J = 8.3 Hz, 1H), 7.59 (d, J = 8.2 Hz, 1H), 7.47 (s, 1H), 6.84−6.44 (m, 12H), 6.07 (d, J = 7.5 Hz, 2H), 5.89 (d, J = 7.4 Hz, 2H), 3.76 (s, 3H). ^{13}C NMR (101 MHz, $CDCl_3$) δ 165.17 (s), 145.37 (s), 144.23 (s), 143.90 (s), 141.38 (s), 135.64 (d, J = 6.7 Hz), 133.64 (s), 133.28 (s), 131.67 (s), 131.12 (s), 123.36 (d, J = 13.2 Hz), 122.34 (s), 121.71 (s), 116.04 (s), 115.71 (s), 113.46 (s), 112.81 (s), 77.38 (s), 77.06 (s), 76.74 (s), 52.81 (s). HRMS (APCI) m/z: $[M + H]^+$ calcd for $C_{32}H_{22}N_2O_4$, 498.1580; found, 499.1644.

Synthesis of MBZ-oPXZ. A mixture of $Pd(OAc)_2$ (44 mg, 0.2 mmol), Cs_2CO_3 (977 mg, 3.0 mmol), (t-Bu)$_3$PHBF$_4$ (88 mg, 0.3 mmol), methyl 2-bromobenzoate (677 mg, 2.7 mmol), and 10H-phenoxazine (458 mg, 2.5 mmol) in toluene (20 mL) was refluxed under N_2 for 48 h. After cooling to room temperature, the reaction mixture was filtered and the residue was purified by column chromatography on silica gel to give a yellow powder (658 mg, yield 83%). Mp: 115−116 °C. ^{1}H NMR (400 MHz, $CDCl_3$) δ 8.15 (d, J = 7.7 Hz, 1H), 7.75 (m, J = 10.7, 4.5 Hz, 2H), 7.56 (t, J = 7.6 Hz, 2H), 7.41 (d, J = 7.7 Hz, 1H), 6.72 − 6.65 (m, 3H), 6.62 (m, J = 10.6, 4.4 Hz, 3H), 6.56 (m, J = 10.8, 4.4 Hz, 3H), 5.78 (d, J = 7.7 Hz, 3H), 3.71 (s, 4H). ^{13}C NMR (101 MHz, $CDCl_3$) δ 165.80 (s), 143.86 (s), 138.53 (s), 134.71 (s), 134.08 (s), 133.35 (s), 133.14 (s), 131.64 (s), 128.88 (s), 123.20 (s), 121.26 (s), 115.42 (s), 112.90 (s), 77.38 (s), 77.07 (s), 76.75 (s), 52.57 (s). HRMS (APCI) m/z: $[M + H]^+$ calcd for $C_{20}H_{15}NO_3$, 317.1052; found, 318.1107.

Synthesis of EBZ-PXZ. A mixture of $Pd(OAc)_2$ (44 mg, 0.2 mmol), Cs_2CO_3 (977 mg, 3.0 mmol), (t-Bu)$_3$PHBF$_4$ (88 mg, 0.3 mmol), ethyl 2-bromobenzoate (616 mg, 2.7 mmol), and 10H-phenoxazine (458 mg, 2.5 mmol) in toluene (20 mL) was refluxed under N_2 for 48 h. After cooling to room temperature, the reaction mixture was filtered and the residue was purified by column chromatography on silica gel to give a yellow powder (679 mg, yield 82%). Mp: 98−99 °C. ^{1}H NMR (400 MHz, $CDCl_3$) δ 8.18 (d, J = 7.7 Hz, 1H), 7.75 (t, J = 7.6 Hz, 1H), 7.57 (t, J = 7.6 Hz, 1H), 7.39 (d, J = 7.7 Hz, 1H), 6.60 (m, J = 22.3, 18.2, 7.5 Hz, 6H), 5.77 (d, J = 7.7 Hz, 2H), 4.15 (q, J = 7.0 Hz, 2H), 1.05 (t, J = 7.0 Hz, 3H). ^{13}C NMR (101 MHz, $CDCl_3$) δ 165.71 (s), 143.75 (s), 137.92 (s), 134.70 (s), 134.20 (s), 133.28 (d, J = 10.4 Hz), 132.21 (s), 128.95 (s), 123.22 (s), 121.15 (s), 115.34 (s), 112.78 (s), 77.37 (s), 77.06 (s), 76.74 (s), 61.60 (s), 13.59 (s). HRMS (APCI): m/z calcd for $C_{21}H_{17}NO_3$ $[M + H]^+$ 331.1208, found 332.1270.

Synthesis of TBZ-PXZ. A mixture of $Pd(OAc)_2$ (44 mg, 0.2 mmol), Cs_2CO_3 (977 mg, 3.0 mmol), (t-Bu)$_3$PHBF$_4$ (88 mg, 0.3 mmol), tert-butyl 2-bromobenzoate (691 mg, 2.7 mmol), and 10H-phenoxazine (458 mg, 2.5 mmol) in toluene (20 mL) was refluxed under N_2 for 48 h. After cooling to room temperature, the reaction mixture was filtered and the residue was purified by column chromatography on silica gel to give a yellow powder (673 mg, yield 75%). Mp: 103−104 °C. ^{1}H NMR (400 MHz, $CDCl_3$) δ 8.07 (d, J = 7.6 Hz, 1H), 7.70 (t, J = 6.9 Hz, 1H), 7.55 (t, J = 7.5 Hz, 1H), 7.35 (d, J = 7.7 Hz, 1H), 6.69−6.53 (m, 6H), 5.79 (d, J = 7.5 Hz, 2H), 1.24 (s, 9H). ^{13}C NMR (101 MHz, $CDCl_3$) δ 165.47 (s), 143.69 (s), 136.75 (s), 134.42 (s), 134.21 (s), 132.82 (s), 132.57 (s), 128.92 (s), 123.31 (s), 121.08 (s), 115.28 (s), 112.76 (s), 82.28 (s), 77.37 (s), 77.05 (s), 76.73 (s), 27.57 (s). HRMS (APCI): m/z calcd for $C_{23}H_{21}NO_3$ $[M + H]^+$ 359.1521, found 360.1570.

■ ASSOCIATED CONTENT

Supporting Information

The Supporting Information is available free of charge at https://pubs.acs.org/doi/10.1021/acsomega.3c02595.

General information, X-ray crystallographic data, symbolic Z-matrix, and ^{1}H NMR and ^{13}C NMR spectra (Figures S1−S12) and crystal data and structure

https://doi.org/10.1021/acsomega.3c02595
ACS Omega 2023, 8, 23142−23147

refinement for **MBZ-oPXZ** and **MBZ-mPXZ** (Tables S1 and S2) (PDF)

AUTHOR INFORMATION

Corresponding Authors

Liang Zhang − *College of Petrochemical Engineering, Longdong University, Qingyang 745000, China;* orcid.org/0009-0005-7865-7939; Email: zhang_liang1113@126.com

Chuan-Feng Chen − *Beijing National Laboratory for Molecular Sciences, CAS Key Laboratory of Molecular Recognition and Function, Institute of Chemistry, Chinese Academy of Sciences, Beijing 100190, China; University of Chinese Academy of Sciences, Beijing 100049, China;* orcid.org/0000-0002-4347-1406; Email: cchen@iccas.ac.cn

Authors

Dingding Yang − *College of Petrochemical Engineering, Longdong University, Qingyang 745000, China*

Quanxing Li − *College of Petrochemical Engineering, Longdong University, Qingyang 745000, China*

Zhi-Jun Li − *College of Petrochemical Engineering, Longdong University, Qingyang 745000, China;* orcid.org/0000-0002-6843-2294

Wen-Bo Zhu − *College of Petrochemical Engineering, Longdong University, Qingyang 745000, China*

Kejian Chang − *College of Petrochemical Engineering, Longdong University, Qingyang 745000, China;* orcid.org/0000-0002-4605-6531

Haiyan Song − *College of Petrochemical Engineering, Longdong University, Qingyang 745000, China*

Complete contact information is available at: https://pubs.acs.org/10.1021/acsomega.3c02595

Notes

The authors declare no competing financial interest.

ACKNOWLEDGMENTS

This work was supported by the Doctoral Start-up Foundsfrom Longdong University (no. XYBY202015), the Youth Science Foundation of Gansu province (nos. 21JR7RM194 and 21JR7RM195), the Young Doctor Fund Projects of Gansu, China (no. 2021QB-119), and the Natural Science Foundation of Qingyang city (no. QY2021A-F010).

REFERENCES

(1) Uoyama, H.; Goushi, K.; Shizu, K.; Nomura, H.; Adachi, C. Highly efficient organic light-emitting diodes from delayed fluorescence. *Nature* **2012**, *492*, 234−238.

(2) Cai, X. Y.; Su, S. J. Marching toward highly efficient, pure-blue, and stable thermally activated delayed fluorescent organic light-emitting diodes. *Adv. Funct. Mater.* **2018**, *28*, No. 1802558.

(3) Liu, Y.; Wu, X.; Chen, Y.; Chen, L.; Li, H.; Wang, S.; Wang, S.; Tian, H.; Tian, H.; Tong, H.; Tong, H.; Wang, L. Triazatruxene-based thermally activated delayed fluorescence small molecules with aggregation-induced emission properties for solution-processable nondoped OLEDs with low efficiency roll-off. *J. Mater. Chem. C* **2019**, *7*, 9719−9725.

(4) Wang, Q.; Tian, Q. S.; Zhang, Y. L.; Tang, X.; Liao, L. S. High-efficiency organic light-emitting diodes with exciplex hosts. *J. Mater. Chem. C* **2019**, *7*, 11329−11360.

(5) Suresh, S. M.; Hall, D.; Beljonne, D.; Olivier, Y.; Zysman-Colman, E. Multiresonant thermally activated delayed fluorescence emitters based on heteroatom-doped nanographenes: recent advances and prospects for organic light-emitting diodes. *Adv. Funct. Mater.* **2020**, *30*, No. 1908677.

(6) Xu, J.; Zhu, X.; Guo, J.; Fan, J.; Zeng, J.; Chen, S.; Zhao, Z.; Tang, B. Z. Aggregation-induced delayed fluorescence luminogens with accelerated reverse intersystem crossing for high-performance OLEDs. *ACS Mater. Lett.* **2019**, *1*, 613−619.

(7) Tao, Y.; Chen, R.; Li, H.; Yuan, J.; Wan, Y.; Jiang, H.; Chen, C.; Si, Y.; Zheng, C.; Yang, B.; Xing, G.; Huang, W. Resonance-activated spin-flipping for efficient organic ultralong room-temperature phosphorescence. *Adv. Mater.* **2018**, *30*, No. 1803856.

(8) Huang, T.; Song, X.; Cai, M.; Zhang, D.; Duan, L. Improving reverse intersystem crossing in exciplex-forming hosts by introducing heavy atom effect. *Today Energy* **2021**, *21*, No. 100705.

(9) Li, Z.; Xu, H.; Yang, D.; Li, Z.; Han, C.; Yang, D.; Zhao, B.; Han, C.; Wang, H.; Zhao, B.; Man, Y.; Wang, H.; Ma, P.; Chang, P.; Ma, D. Optimizing charge transfer and out-coupling of a quasi-planar deep-red TADF emitter: towards rec.2020 gamut and external quantum efficiency beyond 30%. *Angew. Chem., Int. Ed.* **2021**, *60*, 14846−14851.

(10) Ma, M.; Li, J.; Liu, D.; Mei, Y.; Dong, R. Rational utilization of intramolecular hydrogen bonds to achieve blue TADF with EQEs of nearly 30% and single emissive layer all-TADF WOLED. *ACS Appl. Mater. Interfaces* **2021**, *13*, 44615−44627.

(11) Kusakabe, Y.; Wada, Y.; Misono, T.; Suzuki, K.; Shizu, K.; Kaji, H. Imidazole acceptor for both vacuum-processable and solution-processable efficient blue thermally activated delayed fluorescence. *ACS Omega* **2022**, *7*, 16740−16745.

(12) Wu, Z. G.; Han, H. B.; Yan, Z. P.; Luo, X. F.; Wang, Y.; Zheng, Y. X.; Zuo, J. L.; Pan, Y. Chiral octahydro-binaphthol compound-based thermally activated delayed fluorescence materials for circularly polarized electroluminescence with superior EQE of 32.6% and extremely low efficiency roll-off. *Adv. Mater.* **2019**, *31*, No. 1900524.

(13) Liu, H.; Liu, H.; Fan, J.; Guo, J.; Zeng, J.; Qiu, F.; Zhao, Z.; Tang, B. Z. An effective design strategy for robust aggregation-induced delayed fluorescence luminogens to improve efficiency stability of nondoped and doped OLEDs. *Adv. Opt. Mater.* **2020**, *8*, No. 2001027.

(14) Qiu, Z.; Xie, W.; Yang, Z.; Tan, J. H.; Yuan, Z.; Xing, L.; Ji, S.; Chen, W. C.; Huo, Y.; Su, S. J. Nanosecond-time-scale delayed fluorescence towards fast triplet-singlet spin conversion for efficient orange-red OLEDs with negligible efficiency roll-off. *Chem. Eng. J.* **2021**, *415*, No. 128949.

(15) Huang, Z.; Bin, Z.; Su, R.; Yang, F.; Lan, J.; You, J. Molecular design of non-doped OLEDs based on a twisted heptagonal acceptor: a delicate balance between rigidity and rotatability. *Angew. Chem., Int. Ed.* **2020**, *59*, 9992−9996.

(16) Rao, J.; Zhao, C.; Wang, Y.; Bai, K.; Wang, S.; Ding, J.; Wang, L. Achieving deep-blue thermally activated delayed fluorescence in nondoped organic light-emitting diodes through a spiro-blocking strategy. *ACS Omega* **2019**, *4*, 1861−1867.

(17) Liu, Y.; Chen, Y.; Li, H.; Wang, S.; Wu, X.; Tong, H.; Wang, L. High-performance solution-processed red thermally activated delayed fluorescence OLEDs employing aggregation-induced emission-active triazatruxene-based emitters. *ACS Appl. Mater. Interfaces* **2020**, *12*, 30652−30658.

(18) Li, Q.; Hu, J.; Lv, J.; Wang, X.; Shao, S.; Wang, L.; Jing, X.; Wang, F. Through-space charge-transfer polynorbornenes with fixed and controllable spatial alignment of donor and acceptor for high-efficiency blue thermally activated delayed fluorescence. *Angew. Chem., Int. Ed.* **2020**, *59*, 20174−20182.

(19) Xia, G.; Qu, C.; Zhu, Y.; Ye, J.; Ye, K.; Zhang, Z.; Wang, Y. A TADF emitter featuring Linearly Arranged Spiro-Donor and Spiro-Acceptor Groups: Efficient Nondoped and Doped deep-blue OLEDs with CIE_y < 0.1. *Angew. Chem., Int. Ed.* **2021**, *60*, 9598−9603.

(20) Zhang, L.; Wang, Y. F.; Li, M.; Gao, Q. Y.; Chen, C.-F. Quinoline-based aggregation-induced delayed fluorescence materials for highly efficient non-doped organic light-emitting diodes. *Chin. Chem. Lett.* **2021**, *32*, 740−744.

(21) Kim, H. J.; Kang, H.; Jeong, J. E.; Park, S. H.; Koh, C. W.; Kim, C. W.; Woo, H. Y.; Cho, M. J.; Park, S.; Choi, D. H. Ultra-deep-blue aggregation-induced delayed fluorescence emitters: achieving nearly 16% EQE in solution-processed nondoped and doped OLEDs with CIE_y < 0.1. *Adv. Funct. Mater.* **2021**, *31*, No. 2102588.
(22) Matsuo, K.; Yasuda, T. Blue thermally activated delayed fluorescence emitters incorporating acridan analogues with heavy group 14 elements for high-efficiency doped and non-doped OLEDs. *Chem. Sci.* **2019**, *10*, 10687−10697.
(23) Wang, Y.; Zhu, Y.; Lin, X.; Yang, Y.; Zhang, B.; Zhan, H.; Xie, Z.; Cheng, Y. Efficient non-doped yellow OLEDs based on thermally activated delayed fluorescence conjugated polymers with an acridine/carbazole donor backbone and triphenyltriazine acceptor pendant. *J. Mater. Chem. C* **2018**, *6*, 568−574.
(24) Zhao, L.; Wang, S.; Ding, J.; Wang, L. Solution-processible blue fluorescent dendrimers with carbazole/diphenylamine hybrid dendrons for power-efficient organic light-emitting diodes. *ACS Omega* **2019**, *4*, 15923−15928.
(25) Gao, H.; Li, Z.; Pang, Z.; Qin, Y.; Liu, G.; Gao, T.; Dong, X.; Shen, S.; Xie, X.; Wang, P.; Lee, C.-S.; Wang, Y. Rational molecular design strategy for high-efficiency ultrapure blue TADF emitters: symmetrical and rigid sulfur-bridged boron-based acceptors. *ACS Appl. Mater. Interfaces* **2023**, *15*, 5529−5537.
(26) Xu, H.; Zhao, B.; Wang, H.; Han, C.; Ma, P.; Li, Z.; Chang, P. Highly efficient deep-red non-doped diodes based on a T-shape thermally activated delayed fluorescence emitter. *Angew. Chem., Int. Ed.* **2020**, *59*, 19042−19047.
(27) Chen, C.; Lu, H.-Y.; Wang, Y-F.; Li, M.; Shen, Y-F.; Chen, C.-F. Naphthyridine-based thermally activated delayed fluorescence emitters for multi-color organic light-emitting diodes with low efficiency roll-off. *J. Mater. Chem. C* **2019**, *7*, 4673−4680.
(28) Frisch, M. J.; Trucks, G. W.; Schlegel, H. B.; Scuseria, G. E.; Robb, M. A.; Cheeseman, J. R.; Scalmani, G.; Barone, V.; Mennucci, B.; Petersson, G. A.; Nakatsuji, H.; Caricato, M.; Li, X.; Hratchian, H. P.; Izmaylov, A. F.; Bloino, J.; Zheng, G.; Sonnenberg, J. L.; Hada, M.; Ehara, M.; Toyota, K.; Fukuda, R.; Hasegawa, J.; Ishida, M.; Nakajima, T.; Honda, Y.; Kitao, O.; Nakai, H.; Vreven, T.; Montgomery, J. A., Jr.; Peralta, J. E.; Ogliaro, F.; Bearpark, M.; Heyd, J. J.; Brothers, E.; Kudin, K. N.; Staroverov, V. N.; Keith, T.; Kobayashi, R.; Normand, J.; Raghavachari, K.; Rendell, A.; Burant, J. C.; Iyengar, S. S.; Tomasi, J.; Cossi, M.; Rega, N.; Millam, J. M.; Klene, M.; Knox, J. E.; Cross, J. B.; Bakken, V.; Adamo, C.; Jaramillo, J.; Gomperts, R.; Stratmann, R. E.; Yazyev, O.; Austin, A. J.; Cammi, R.; Pomelli, C.; Ochterski, J. W.; Martin, R. L.; Morokuma, K.; Zakrzewski, V. G.; Voth, G. A.; Salvador, P.; Dannenberg, J. J.; Dapprich, S.; Daniels, A. D.; Farkas, O.; Foresman, J. B.; Ortiz, J. V.; Cioslowski, J.; Fox, D. J. *Gaussian 09*, revision D.01; Gaussian, Inc.: Wallingford CT, 2013.

https://doi.org/10.1021/acsomega.3c02595
ACS Omega 2023, 8, 23142−23147